PACOSYT: A Passive Component Synthesis Tool Based on Machine Learning and Tailored Modeling Strategies Towards Optimal RF and mm-Wave Circuit Designs

FÁBIO PASSOS [1] **(Senior Member, IEEE), NUNO LOURENÇO** [1,2] **(Member, IEEE), ELISENDA ROCA** [3],
RICARDO MARTINS [1,4] **(Member, IEEE), RAFAEL CASTRO-LÓPEZ** [3],
NUNO HORTA [1,4] **(Senior Member, IEEE), AND FRANCISCO V. FERNÁNDEZ** [3]

(Regular Paper)

[1]Instituto de Telecomunicações, 1049-001 Lisboa, Portugal
[2]Universidade de Évora, 7004-516 Évora, Portugal
[3]Instituto de Microelectrónica de Sevilla, Universidad de Sevilla - CSIC, 41092 Seville, Spain
[4]Instituto Superior Técnico, Universidade de Lisboa, 1049-001 Lisboa, Portugal

CORRESPONDING AUTHOR: Fábio Passos (e-mail: fabio.passos@lx.it.pt).

ABSTRACT In this paper, the application of regression-based supervised machine learning (ML) methods to the modeling of integrated inductors and transformers is examined. Different ML techniques are used and compared to improve accuracy. However, it is demonstrated that none of the ML techniques considered provided good results unless a smart modeling strategy, tailored to the specific design problem, is used. Taking advantage of these modeling strategies, high accuracy can be obtained when compared to full-wave electromagnetic (EM) simulations (less than 2% error) and experimental measurements (less than 5% error). The most accurate model, obtained by the appropriate combination of an ML technique and modeling strategy, has been integrated into a tool called PACOSYT. The tool uses optimization algorithms to allow the designer to obtain an inductor/transformer with optimal performances in just seconds while keeping the accuracy of EM simulations. Furthermore, the tool provides the passive component S parameter description file for seamless use in circuit simulations. The tool can be used standalone or integrated with design frameworks, like Cadence Virtuoso or AIDASoft, a framework for circuit optimization. To illustrate the different usages of the tool, several passive devices are synthesized, and hundreds of millimeter-wave power amplifiers are synthesized using AIDASoft together with PACOSYT. The tool has been developed using open-source Python frameworks and does not use any closed-source licenses. PACOSYT, which also allows other designers to create their models for different technologies, is made publicly available.

INDEX TERMS Design automation, inductors, integrated circuits, machine learning, millimeter-wave, modeling, radio-frequency, synthesis, transformers.

I. INTRODUCTION

Passive devices such as inductors and transformers are one of the biggest bottlenecks in radio-frequency (RF) and millimeter-wave (mm-Wave) circuit design due to the lack of accurate and fast performance evaluation techniques [1].

Usually, RF and mm-Wave designers depend on electromagnetic (EM) simulators to accurately predict such devices' performances. As an alternative to the time-consuming EM simulations, analytical models appeared as quicker-to-evaluate solutions, both for inductors [2], [3], [4]

and transformers [5], [6], [7]. However, such models do not provide the desired accuracy, especially in the multi-gigahertz frequency range. For instance, the lumped-element p-model for inductors reported in [3] can predict the performances of the passive structures with acceptable accuracy, but only up to a couple of GHz. A more complex 2p-model was also applied to inductors in [4]; however, its parameters are derived from analytical equations and fitting parameters, and thus, such models are not easily scalable. On the other hand, the modeling of transformers is significantly more challenging than inductor modeling because, in addition to the interaction between windings, there is also the interaction between the transformer's primary and secondary coils. Models with higher complexity have been developed for transformers [5], [6], [7], but these still have some deficiencies: either they do not take into account some magnetic coupling effects between the windings (hence losing accuracy), or they need prior fabrication to extract the model parameters (hence complicating the modeling process). Moreover, the accuracy of these models is always evaluated against a few inductor/transformer samples and without a detailed error analysis. Also, most analytical models are only valid in a quite limited region of the design space (i.e., range of geometrical parameters of the inductor/transformer), compromising simulation accuracy outside those regions. Furthermore, lumped-element analytical models struggle to be wideband (e.g., from around DC up to multi-GHz), and, therefore, their usage in RF and/or mm-Wave circuit design may be limited.

In the past two decades, surrogate modeling, a kind of supervised machine learning, has emerged as a possible solution to the problem of how to accurately evaluate passive components in substantially shorter execution times than EM simulations [8], [9], [10], [11], [12], [13], [14], [15], [16], [17], [18], [19], [20], [21], [22], [23], [24], [25], [26], [27]. Moreover, a very extensive survey of recent advances in the area is available in [28]. The work presented here studies the performance of several ML regression techniques for generating surrogate models of inductors and transformers. It also demonstrates how the use of different modeling strategies that exploit specific knowledge of the RF design problem is necessary to improve the accuracy of such models, although leading to different accuracy results depending on the ML technique used. The models developed in this work aim to support RF/mm-Wave IC designers and, therefore, an open-source tool named PACOSYT was created. It allows the user to design/synthesize inductors and transformers and create other models for different component topologies or technologies. The tool can be used standalone or integrated with design frameworks, such as Cadence Virtuoso [29] for manual circuit design or AIDASoft [30], [31], a framework for circuit optimization. The tool was developed in Python coding language using only open-source libraries. PACOSYT is available online in [32].

The remainder of this paper is organized as follows. Section II briefly defines the problem by outlining the main inductor/transformer design parameters and performances.
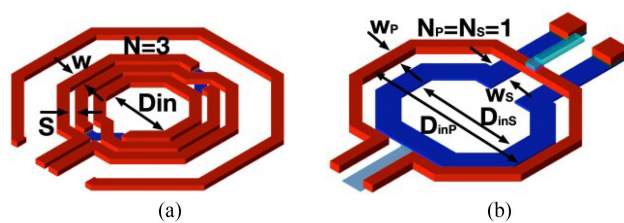

FIGURE 1. Layout of a 3-turn inductor (with guard ring) and a 1:1 transformer with their geometric parameters annotated.

Section III explains how surrogate models are generated, discussing the different approaches to create them, and introducing the ML techniques used in this work. In Section IV, different strategies are applied to the modeling of inductors and transformers in two different technologies, and the most effective combination of modeling strategy and ML regression technique is identified and selected for usage in the remainder of the paper. In Section V, PACOSYT's capabilities and graphical user interface (GUI) are presented. In Section VI, hundreds of mm-Wave power amplifiers (PA) working at 28 GHz are automatically designed using AIDAsoft and PACOSYT. Finally, in Section VII, conclusions are drawn.

II. MODELING PROBLEM DEFINITION

For both inductors and transformers, the designer is usually interested in obtaining a given coil inductance at the operation frequency ($f0$), with the highest quality factor and the smallest area. Additionally, the coupling factor must also be considered for transformers. Therefore, the objective of an inductor/transformer model should be the capability of providing the component performances of interest given a particular geometry. In this section, the main geometrical parameters that define both inductor and transformer devices are presented as well as their main performances.

A. INDUCTOR AND TRANSFORMER GEOMETRICAL PARAMETERS

Fig. 1(a) shows an octagonal symmetric inductor, and Fig. 1(b) shows an octagonal symmetric transformer. The design space of inductors is given by its geometry, which is usually defined by four geometric parameters: the number of turns (N), inner diameter (Din), turn width (w), and spacing between turns (s). For the transformers, eight geometric parameters are used: the number of turns of primary (NP) and secondary (NS), the inner diameter of the primary (DinP) and secondary (DinS), the turn width of the primary (wP) and secondary (wS) and finally, the spacing between turns of the primary (sP) and secondary (sS). In this work, the spacing between turns is kept constant for all devices at the minimum value allowed by the technology because the highest quality factors are usually obtained in such a way.

B. INDUCTOR AND TRANSFORMER PERFORMANCE PARAMETERS

The inductance, L, and the quality factor, Q, are the most relevant inductor performances. In Fig. 2, a plot of L and Q
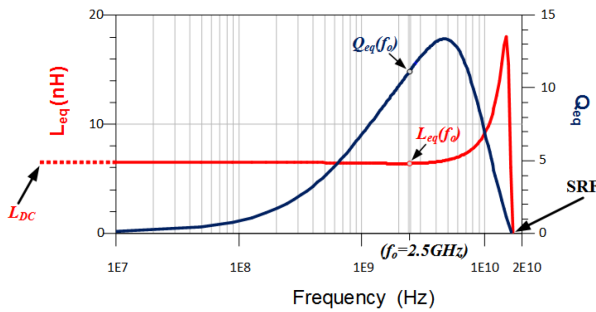
FIGURE 2. Illustrating inductors/transformers performance parameters. Inductance and quality factor vs frequency curves.

as a function of the frequency is shown. Similarly, for the transformers, the performances of interest are the inductance of the primary and secondary coils, LP and LS, respectively, and the quality factor of the primary and secondary coils, QP and QS, respectively. Also, the coupling factor k between coils is an important design parameter for the transformers, especially for mm-Wave circuit design. These performance figures can be calculated from the S-parameters and depend on how the inductor/ transformer is excited (e.g., single-ended or differential excitation) [33]. Another important parameter is the self-resonance frequency, SRF, which is defined as the frequency at which the behavior of the inductor/transformer changes from inductive to capacitive. Therefore, if the inductor operates close to the SRF, its inductance value can change significantly due to process variability (see the inductance curve in Fig. 2 near the SRF). Hence, the SRF is not a design goal per se, but designers are usually interested in knowing its frequency location to stay away from it. There are two self-resonance frequencies in the specific case of transformers (one for each coil): the primary SRFP and the secondary SRFS.

In this work, the S-parameter real and imaginary parts are modeled. The advantages of modeling the S-parameters instead of the performance parameters (i.e., L and Q) are the following:

1) The model becomes general and valid for both single-ended and differential excitation;
2) The model can be directly used to create S-parameter files that can be used in modern circuit simulators seamlessly.

However, since inductance, quality factor and coupling factor are the meaningful measures the designer is searching for, the error evaluation of the modeling techniques in the next section is performed in the performance parameters for the differential excitation case. For an inductor, which is a 2-port structure, it is necessary to first convert the 2-port structure to a 1-port differential structure [34]. Correspondingly, for a transformer, a 4-port structure (6-port if we consider the center taps) the first step in calculating the performances is to convert from a 4-port S-parameter description to a 2-port differential S-parameter description [34], Then, the equivalent impedance representation can be obtained and from it, the inductor/transformer performances can be obtained.

III. SURROGATE MODELS
The objective of a surrogate model is to mimic the output response of a given system based on some inputs. To create a surrogate model, it must first learn how the system behaves from a set of input samples (known as the training samples or training set); and then, it will be able to predict the behavior of new samples. Hence, three steps must be performed to create a surrogate model: design of experiments (DOE), model creation, and model validation. First, in the DOE, the design space is sampled to create the training set from which the model will learn. Ideally, models should learn from the most accurate evaluation possible, which in this case are full-wave EM simulations performed with ADS Momentum [35]. Second, the model is created with a given technique (i.e., Gaussian process, artificial neural networks, radial basis function, among others), and third, in the end, the model is validated using a test set (with different samples from the ones used for training).

The first decision to make is selecting the modeling approach to follow, that is, which type of model the specific problem at hand requires: a global model or a local model built with surrogate-assisted approaches. Some authors propose the creation of a global model that is valid and accurate in the entire design space of the passive component under study and can later be used as a performance predictor or as a performance evaluator in optimization procedures [9], [17], [24]. In those approaches, the training samples are generated a priori covering the entire design space, and the model is built based on those training samples. The generation of the training samples may also be considered part of the approach. Such generation is time-consuming and knowing a priori the number of necessary samples to develop accurate models is by no means trivial. Therefore, adaptive sampling algorithms have been proposed [10]. The main idea of such algorithms is to create a small number of training samples, create the model and assess its accuracy. Then, more samples are added iteratively to the training set while assessing the model's accuracy until the desired accuracy is reached.

Instead of creating a model valid for the entire design space, other authors prefer to design a component with a set of performances within an optimization loop, i.e., these strategies are intended for designing a device with some specific performances instead of obtaining a widely applicable model. The model is simultaneously constructed during the design process and only creates an (hopefully) accurate model around the optimal region (i.e., the model is local). In this category, we include the surrogate-assisted (SA) models [11], [23] or space-mapping techniques with adaptive surrogate models [8]. A coarse model using a few training points is first built on them. Then, this coarse model is coupled with an optimization algorithm, and promising solutions (typically one) are electromagnetically simulated at each iteration of the optimization loop. The data from this EM simulation is used to update the model, improving its accuracy in the region where new simulation points are added while moving towards the presumed optimal structure. However, there are two fundamental

limitations to these approaches. First, the promising solutions found at the different iterations constrain the search space, and the constructed model is accurate only in that space. Second, the success of such surrogate-assisted approaches comes from the basic assumption that the optimal point of the coarse and the fine models are not far away in the design space. However, this assumption only holds when the coarse model is accurate enough.

In this work, since the objectives of the developed model are to be used by designers in a design framework (e.g., Cadence Virtuoso), similarly as models provided by a foundry process design kit (PDK) would be used, as well as be used as a performance evaluator in circuit optimization, the model must be valid in the entire design space. Therefore, the global approach will be considered for the model creation.

Most reported surrogate models are based on general supervised ML methods that have not been explicitly created to model integrated passive components. Besides, their applicability is not always straightforward. Hence, among all the possibilities that ML techniques allow for, to accurately model a given passive structure, two choices/questions must be made/answered:

1) Which ML technique to use (e.g., Gaussian process, artificial neural network, etc.);
2) Which strategy to consider for model creation that exploits knowledge of passive device performances (e.g., which should be the inputs/outputs of the model).

Regarding the first choice, there are several ML techniques proposed in the literature and applied to passive component modeling [8], [9], [10], [11], [12], [13], [14], [15], [16], [17], [18], [19], [20], [21], [22], [23], [24], [25], [26], [27], [28]. The following ones are considered in this work: Gaussian-process regression (GPR), kernel ridge regression (KRR), random forest regression (RFR), radial basis function (RBF), nearest neighbor (NN), and ANNs. The detailed description of these techniques is out of the scope of this work and detailed information can be found in dedicated ML literature, such as [36], [37].

Finally, regarding the second choice, the problem-specific modeling strategy, it is crucial to understand the modeling problem at hand to develop a strategy that improves model accuracy. The strategy encompasses the selection of the adequate input parameters and any specific behavior of the components under study that can be used to improve its accuracy further. Several strategies will be considered in the following Section, and applied to create surrogate models using the six ML techniques proposed before. A comprehensive one is proposed that, combined with the appropriate ML technique, provides highly accurate modeling.

IV. INDUCTOR AND TRANSFORMER MODELING STRATEGIES

This work aims to get a model for circuit designers that can be used in several applications. Therefore, the goal is to develop a model that is:

- Highly accurate;

TABLE 1. Design Space for the Inductors and Transformers

Structure	N	D_{in} (µm)	w (µm)
Inductors	1~5	60~200	5~15
Transformers	N_P / N_S	D_{inP} / D_{inS}	w_P / w_S
	1~2	30~200	5~15

- Computationally efficient, i.e., with drastically shorter execution times than EM simulations;
- Valid in the entire design space of interest so that it can generally be used in typical design procedures (e.g., as the PDK models from semiconductor foundries) and also usable for automated synthesis procedures;
- Wideband (valid from DC up to the mm-Wave regime);
- Capable of being used in electrical circuit simulation;
- Valid for single-ended and differential excitations.

In this paper, for the inductors, a 0.35-µm technology was considered, and for the transformers, a 65-nm technology was considered. However, the techniques presented in this work are technology agnostic. The range for each input variable (geometric parameters of inductors/transformers) is defined as shown in Table 1. This design space was sampled using a Quasi-Monte-Carlo technique [36]. To create the models, 500 training samples are used for inductors, and 3000 training samples are used for transformers. More samples are used to train the transformer model because these structures have twice the input parameters, which considerably increases the size of their design space. For the statistical validation of the models, a test set was generated with new samples of the same design space: 150 samples for the inductors and 300 for the transformers.

Throughout this section, the considered strategies go from more general approaches to more tailored ones, improving the model error and finally reaching a combination of technique and strategy which can provide a model that complies with all the above points. All experiments in this paper were conducted in an Intel i7 Quad-Core with 32GB of RAM.

A. FREQUENCY-DEPENDENT MODEL

Inductors and transformers are components whose performances are inherently frequency-dependent (FD). Therefore, the first strategy (Strategy I) employed is to build the models with the frequency as an input of the model (as well as the component geometrical parameters). Accordingly, its input parameters, x_m, are:

$$x_m = \left[f, x_v \right]^T = \left[f, x_1, x_2, \ldots, x_d \right]^T \tag{1}$$

where f is the frequency, and d is the length of the design variables' vector, x_v, e.g., for the inductor model x_v is composed of N, Din and w, whereas for the transformer, x_v is composed of NP, NS, DinP, DinS, wP, and wS. The output parameters of the model, y_m, correspond to a set of values:

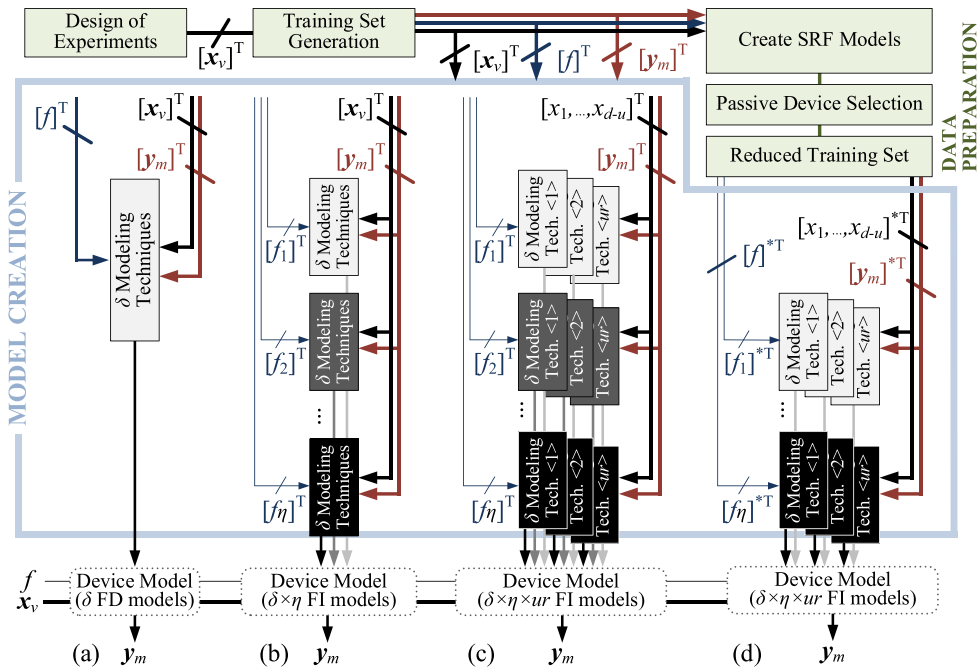$$y_m = \left[y_1, y_2, \ldots, y_t \right]^T \tag{2}$$

FIGURE 3. Illustrating the model strategies employed in this work.

TABLE 2. Statistical Study for the Different Modeling Techniques for the Frequency-Dependent Modeling Strategy

Strategy I		Technique										
FD Model		GPR		KRR		RBF		RFR		NN		ANN	
Structure	Performance	ME (%)	MAPE (%)	ME (%)	MAPE (%)	ME (%)	MAPE (%)	ME (%)	MAPE (%)	ME (%)	MAPE (%)	ME (%)	MAPE (%)
Inductors (5GHz)	L	n/a	n/a	n/a	n/a	919.94	52.41	262.9	6.43	188.35	6.11	281.8	5.85
	Q	n/a	n/a	n/a	n/a	4503.3	123.91	332.17	9.98	188.36	8.03	335.95	14.08
Transformers (28GHz)	L_P	n/a	n/a	n/a	n/a	325.92	86.75	81.53	8.33	121.71	42.49	145.84	5.82
	Q_P	n/a	n/a	n/a	n/a	218.66	103.63	87.76	17.81	4734.25	418.82	184.71	26.73
	L_S	n/a	n/a	n/a	n/a	10671.42	303.86	1815.32	37.16	6088.05	139.35	808.26	22.17
	Q_S	n/a	n/a	n/a	n/a	2263.12	165.57	2528.58	58.84	25199.16	759.65	925	39.02
	k	n/a	n/a	n/a	n/a	1689.02	235.61	81.98	9.88	171.1	53.16	290.53	14.69

where t is the total number of S-parameter components of the different passive devices. The creation of this model is illustrated in Fig. 3(a).

FD models were created using the technique described in Section VII. To have a complete frequency description of the passive components, the objective was to model from 1 MHz up to 200 GHz using 200 frequency points. The results can be seen in Table 2. Although the model is created for the entire frequency range, regarding the error evaluation, only two frequency points were chosen: 5 GHz for the inductors and 28 GHz for the transformers. It is possible to observe in Table 2 that both the maximum error (ME) and the mean absolute percentage error (MAPE) are catastrophic for every technique, with errors of more than 25000% for some techniques. Notice that although a specific sample could show a reduced modeling error, the ME and MAPE metrics are calculated statistically over hundreds of devices and are therefore, representative of the global applicability of the model.

Apart from the significant error reported, the GPR and KRR models were unable to be created. This happened as all 200

frequency points are used as inputs to the model (to have a decent frequency description of the passive), and therefore the dataset becomes extremely large. Hence, the GPR and KRR techniques require a considerable amount of memory (e.g., 3.6 Terabytes of memory for the KRR technique), and it becomes impossible to build FD models using such techniques (in these conditions). Logically, the number of frequency points and/or the maximum frequency could be decreased to reduce the dataset size but at the expense of losing precision in the frequency behavior of the component. However, this fact would impact the accuracy later on during circuit simulation. Since the model must be wideband and usable in circuit simulations, this is already a downside of the FD strategy if a model such as GPR or KRR is to be used.

Since the model cannot be built with some techniques, and the trainable one's present huge errors, it is possible to conclude that using the frequency as an input variable is not a viable strategy to model inductors and transformers accurately. Also, the training time of the FD models is high (in the range of hours for some techniques).

TABLE 3. Statistical Study for the Different Modeling Techniques for the Frequency-Independent Modeling Strategy

Strategy II		Technique											
FI Model		GPR		KRR		RBF		RFR		NN		ANN	
Structure	Performance	ME (%)	MAPE (%)	ME (%)	MAPE (%)	ME (%)	MAPE (%)	ME (%)	MAPE (%)	ME (%)	MAPE (%)	ME (%)	MAPE (%)
Inductors (5GHz)	L	369.49	13.26	102.72	54.82	10.16	0.22	346.95	6.59	188.35	6.11	19.02	1.10
	Q	277.15	53.34	113.93	95.59	10.17	0.77	388.21	8.29	188.36	8.03	24.21	4.87
Transformers (28GHz)	L_P	15.90	0.46	18.91	2.41	8.37	0.34	27.17	4.49	121.71	42.49	12.67	2.51
	Q_P	17.50	1.74	200.71	15.63	8.69	1.32	58.15	10.79	4734.25	418.82	72.97	10.99
	L_S	40.45	1.31	248.25	6.4	16.34	0.72	742.15	18.02	6088.05	139.35	597.58	12.69
	Q_S	42.54	2.35	190.05	15.43	16.92	1.64	774.93	25.39	25199.16	759.65	566.16	16.33
	k	29.79	0.84	47.9	3.22	8.52	0.41	167.96	8.35	171.1	53.16	58.83	2.91

B. FREQUENCY-INDEPENDENT MODEL

The following strategy (Strategy II) is to remove the frequency from the models' input and train η frequency-independent (FI) sub-models, one for each frequency point sampled during EM simulation, i.e., 200 in the current trial. Accordingly, the set of inputs for the η sub-models are:

$$(\boldsymbol{x}_m)_{\langle \eta \rangle} = \left([\boldsymbol{x}_v]^T \right)_{\langle \eta \rangle} = \left([x_1, x_2, \ldots, x_d]^T \right)_{\langle \eta \rangle} \quad (3)$$

Similarly, the output parameters of the η models are:

$$(\boldsymbol{y}_m)_{\langle \eta \rangle} = \left([y_1, y_2, \ldots, y_t]^T \right)_{\langle \eta \rangle} \quad (4)$$

This strategy is illustrated in Fig. 3(b). The model errors are shown in Table 3. It is possible to conclude that all techniques can be used by removing the frequency from the inputs. The ME improves in all techniques by at least an order of magnitude, proving that this strategy is more effective than the FD models. The NN is the only technique that maintains its errors because the model is built using the nearest training sample, which does not change from Strategy I to Strategy II. Some techniques present very low MAPEs (e.g., RBF), which could be considered a reasonable accuracy. However, the MEs of such techniques are still too high to consider these models usable for circuit design, and therefore another strategy must be explored. The training time of the FI models is less than the previous technique but still time-consuming (in the range of tens of minutes).

C. FREQUENCY-INDEPENDENT PER-TURN MODEL

Since the number of turns in a passive device is a discrete value, typically with very few choices, and, additionally, it drastically changes the component's behavior, removing the number of turns as input of the model is a tempting strategy. Therefore, the next strategy (Strategy III) is to create a sub-model for each different number of turns (or combination of turns for transformers, for instances different models for e.g., 2:1 or 1:2 turn combination). Starting with the FI sub-models of (3) and (4), $\eta \times ur$ per-turn sub-models are trained, with ur being the amount of number of turns possible for a given passive device, e.g., 1-turn, 2-turns, etc., for inductors. The models' input is:

$$\left\{ (\boldsymbol{x}_m)_{\langle \eta \rangle} \right\}_{\langle ur \rangle} = \left\{ \left([\boldsymbol{x}_{v-u}]^T \right)_{\langle \eta \rangle} \right\}_{\langle ur \rangle}$$

$$= \left\{ \left([x_1, x_2, \ldots, x_{d-u}]^T \right)_{\langle \eta \rangle} \right\}_{\langle ur \rangle} \quad (5)$$

with u being the number of turn-related variables on $\boldsymbol{x}_v$ for each passive device, i.e., for the inductor previously described in Section II is one, N, whereas for the transformer are two, NP and NS. Accordingly, the $\eta \times ur$ models' output parameters are:

$$\left\{ (\boldsymbol{y}_m)_{\langle \eta \rangle} \right\}_{\langle ur \rangle} = \left\{ \left([y_1, y_2, \ldots, y_t]^T \right)_{\langle \eta \rangle} \right\}_{\langle ur \rangle} \quad (6)$$

This approach is illustrated in Fig. 3(c), and the results obtained by it can be observed in Table 4. It is possible to perceive that this strategy allows to highly reduce the inductor MEs and MAPEs, with some modeling techniques attaining MEs lower than 1% for inductors with a lower number of turns and also 1:1 transformers. However, when the number of turns increases (i.e., N=5 inductors or 1:2 transformers) the errors are still too high to consider this strategy usable since ME values up to 30% still occur for some modeling techniques. Regarding the training time of the FI per-turn models, it is extremely fast for all techniques (in the range of seconds).

D. FREQUENCY-INDEPENDENT PER-TURN SRF–FILTERED MODEL

As previously said, when the number of turns increases, both the ME and MAPE increase. However, it is impossible to perform further design space partition by creating more sub-models straightforwardly. Therefore, the specific behavior of the component under study plays a vital role in improving the model accuracy.

The error increase for components with a high number of turns can be explained because some passives from the training set have their SRF (SRFP or SRFS for transformers) below or around the frequency where the error is being evaluated. Most ML techniques assume smooth behaviors, i.e., if an input variable changes by a small amount, the output varies smoothly. However, this is not the case for the S-Parameters (and consequently L and Q) if the training inductors/transformers have their SRF close to the operation frequency (Fig. 2). Thus, using these inductors/transformers in the model construction dramatically decreases the model's accuracy for test inductors/ transformers with SRF above the frequency of operation. Potentially useful inductors/transformers

TABLE 4. Statistical Study for the Different Modeling Techniques for the Frequency-Independent Per Turn Modeling Strategy

Strategy III			Technique										
FI Per-Turn Model			GPR		KRR		RBF		RFR		NN		ANN	
Structure	Performance		ME (%)	MAPE (%)	ME (%)	MAPE (%)	ME (%)	MAPE (%)	ME (%)	MAPE (%)	ME (%)	MAPE (%)	ME (%)	MAPE (%)
Inductors (5GHz)	N=1	L	0.20	0.06	0.19	0.06	0.16	0.05	4.82	1.55	5.62	1.14	0.60	0.16
		Q	3.27	1.01	1.50	0.55	0.57	0.15	12.48	4.47	18.65	5.59	3.31	0.60
	N=2	L	0.10	0.04	0.12	0.04	0.11	0.03	4.87	2.18	6.33	1.35	0.70	0.20
		Q	1.33	0.39	1.46	0.44	0.23	0.06	10.73	4.45	15.75	4.83	5.03	0.77
	N=3	L	0.10	0.03	0.12	0.03	0.18	0.04	6.02	2.16	5.59	1.41	1.15	0.25
		Q	0.83	0.29	1.05	0.31	0.32	0.05	12.09	4.54	10.68	2.84	8.82	1.80
	N=4	L	0.08	0.04	0.23	0.04	0.15	0.05	8.95	3.03	8.65	2.69	2.51	0.50
		Q	0.86	0.18	1.36	0.24	0.62	0.12	17.23	4.29	13.88	3.39	13.13	2.20
	N=5	L	37.80	1.92	20.73	1.40	40.58	1.98	1698.49	97.05	2366.15	112.67	328.75	14.58
		Q	37.84	2.01	20.88	1.49	41.37	2.13	1952.25	122.50	2794.11	173.28	332.95	16.74
Transformers (28GHz)	N=1:1	L_P	0.23	0.12	1.04	0.22	0.35	0.16	11.86	2.03	10.62	3.61	1.31	0.41
		Q_P	3.84	1.38	4.86	1.81	3.77	1.53	15.16	7.44	21.78	4.33	42.63	4.89
		L_S	0.26	0.1	1.03	0.31	0.24	0.08	12.06	3.6	10.15	4.22	1.62	0.53
		Q_S	7.17	1.98	12.32	4.04	2.2	0.78	14.29	6.73	12.8	4.7	17.05	4.28
		k	0.55	0.18	0.81	0.25	0.45	0.21	18	5.33	25.38	9.02	2.93	0.76
	N=1:2	L_P	8.8	0.59	30.06	1.72	13.46	0.89	17.92	3.07	151.58	11.4	33.46	2.38
		Q_P	10.27	2.65	31.44	3.99	16.08	3.22	55.39	13.97	167.15	20.39	68.16	6.74
		L_S	17.11	1.04	57.35	3.11	26.82	1.58	23.3	6.54	258.33	20.09	69.32	4.74
		Q_S	18.06	2.3	57.39	5	28.42	3.52	43.79	10.42	355.21	27.44	107.44	11.2
		k	3.77	0.42	17.56	1.28	6.12	0.66	14.84	5.96	280.66	24.72	8.59	1.23
	N=2:1	L_P	0.93	0.33	1.21	0.41	0.81	0.33	26.31	8.88	40.98	15.4	3.61	1.68
		Q_P	2.41	0.72	4.2	1.29	2.81	1.09	45.25	14.59	181.1	24.22	23.8	6.43
		L_S	26.18	1.35	25.98	1.55	39.28	1.94	1224.25	56.96	848.32	57.74	28.65	2.75
		Q_S	27.56	2.31	27.72	3.27	41.31	2.98	1418.06	71.21	1300.62	72	27.55	5.66
		k	16.51	0.89	16.5	1.08	28.52	1.45	76.5	10.8	71.78	16.43	18.47	2.03

have their SRF sufficiently above the frequency of operation. The accuracy estimation of inductance and quality factor of these useful devices is dramatically increased if only devices with SRF sufficiently above the operating frequency are used for model training. Therefore, the strategy proposed here (Strategy IV) is outlined in Algorithm 1 and based on a two-step method:

Generate models capable of predicting the SRF values (for each number of turns) using all training inductors, and SRFP and SRFS using all training transformers (line 8 of Algorithm 1);

To generate highly accurate models for the S-parameters, only those components from the training set whose SRF (or SRFP and SRFS) is sufficiently above the operating frequency, f0, are used (line 7 of Algorithm 1). For example, if the operating frequency is 5 GHz, only components with SRF>6 GHz ($\Delta f = 1$ GHz) are used to generate the S-parameter models.

Consequently, with this methodology, whenever a test component is going to be evaluated, its SRF value is predicted first (line 15 of Algorithm 1). If the predicted SRF is below e.g., 6 GHz, the component is discarded since it is not useful for the selected operating frequency. Otherwise, its inductance and quality factor are calculated using the S-parameter models. The creation of the models using the proposed strategy is illustrated in Fig. 3(d).

The accuracy of the results using this strategy can be seen in Table 5 It can be concluded that it is possible to achieve very low ME and MAPE for several techniques, some of them with

ME lower than 5% and MAPE lower than 2% when compared to full-wave EM simulations, which proves to be a highly accurate modeling strategy. Regarding the SRF models, the most accurate technique is the RBF, which achieves MAPEs of around 2% for inductors and around 4.4% for transformers. Regarding the training time of these models, it is similar to the previous strategy (in the range of seconds for most techniques).

### E. MODELING ACCURACY COMPARISON

Regarding the strategy, it is easy to conclude that the most accurate one is Strategy IV, the FI per-turn SRF-filtered modeling strategy. Perhaps the strategy accuracy enhancement is more visible if a comparison is made for the error of the NN technique (the most basic technique) between the initial strategy presented in Table 2 and the final strategy presented in Table 5. It is possible to conclude that it was possible to reduce the error in several orders of magnitude, from around 25000% to 36% ME, which is a huge improvement when considering that the modeling technique is the same, but only the strategy changed. Regarding the RBF technique (one of the most accurate ones), the improvements are from around 1700% to 0.57% ME, with MAPEs going from 70% to 0.15% between both strategies. Regarding the model technique, three models have proven to have the best accuracy: the GPR, KRR and RBF. Although they have comparable accuracy, it appears that the RBF showed the lowest MAPE for the overall set of different components. Therefore, in summary, the RBF

TABLE 5. Statistical Study for the Different Modeling Techniques for the FI Per-Turn SRF-filtered Modeling Strategy

Strategy IV			Technique										
FI Per-Turn SRF-filtered Model			GPR		KRR		RBF		RFR		NN		ANN	
Structure	Performance		ME (%)	MAPE (%)	ME (%)	MAPE (%)	ME (%)	MAPE (%)	ME (%)	MAPE (%)	ME (%)	MAPE (%)	ME (%)	MAPE (%)
Inductors (5GHz)	N=1	L	0.20	0.06	0.19	0.06	0.16	**0.05**	4.82	1.55	5.62	1.14	0.60	0.16
		Q	3.27	1.01	1.50	0.55	0.57	**0.15**	12.48	4.47	18.65	5.59	3.31	0.60
	N=2	L	0.10	0.04	0.12	0.04	0.11	**0.03**	4.87	2.18	6.33	1.35	0.70	0.20
		Q	1.33	0.39	1.46	0.44	0.23	**0.06**	10.73	4.45	15.75	4.83	5.03	0.77
	N=3	L	0.10	0.03	0.12	0.03	0.18	**0.04**	6.02	2.16	5.59	1.41	1.15	0.25
		Q	0.83	0.29	1.05	0.31	0.32	**0.05**	12.09	4.54	10.68	2.84	8.82	1.80
	N=4	L	0.09	0.03	0.10	0.03	0.15	**0.04**	5.94	2.14	5.09	1.99	2.42	0.48
		Q	0.40	0.14	0.60	0.17	0.27	**0.08**	6.63	2.92	8.81	2.27	6.57	1.40
	N=5	L	0.10	0.05	0.10	0.05	0.08	**0.05**	17.47	6.11	14.57	5.24	4.67	0.81
		Q	0.52	0.17	0.92	0.26	0.15	**0.05**	21.43	5.46	18.05	4.50	39.70	4.96
Transformers (28GHz)	N=1:1	L_P	0.23	0.12	1.04	0.22	0.35	**0.16**	14.24	2.47	10.62	3.35	2.30	0.50
		Q_P	3.84	1.38	4.86	1.81	3.77	**1.53**	22.11	9.14	22.14	4.47	139.36	7.82
		L_S	0.26	0.1	1.03	0.31	0.24	**0.08**	13.09	4.46	16.44	5.61	2.89	0.65
		Q_S	7.17	1.98	12.32	4.04	2.2	**0.78**	16.65	7.90	34.18	9.71	30.19	4.05
		k	0.55	0.18	0.81	0.25	0.45	**0.21**	28.18	6.56	25.38	8.87	5.84	1.08
	N=1:2	L_P	0.57	0.14	0.48	0.15	0.53	**0.17**	12.03	2.94	11.92	3.88	1.63	0.66
		Q_P	4.59	1.78	5.41	1.84	5.28	**1.94**	25.51	13.93	27.33	8.39	28.16	5.06
		L_S	0.39	0.16	0.46	0.22	0.53	**0.17**	15.93	4.84	19.21	7.26	2.74	0.80
		Q_S	4.73	1.21	3.53	1.48	4.55	**1.49**	16.64	7.93	19.95	5.24	18.91	4.31
		k	0.77	0.25	1.15	0.46	0.84	**0.28**	39.20	9.14	34.19	12.82	3.17	1.09
	N=2:1	L_P	0.16	0.14	0.29	0.22	0.06	**0.05**	12.58	6.87	36.05	10.18	2.26	1.40
		Q_P	1.63	1.13	1.54	0.9	0.71	**0.36**	18.37	9.83	31.87	10.65	15.53	7.34
		L_S	0.62	0.44	1.09	0.96	0.1	**0.07**	13.04	4.87	12.96	6.08	2.64	1.01
		Q_S	5.83	4.04	6.76	5.14	1.85	**0.97**	20.57	10.80	29.00	13.96	8.68	3.43
		k	0.5	0.43	1.1	0.82	0.4	**0.25**	18.07	10.56	35.74	13.40	2.69	0.89

Algorithm 1: Frequency-Independent Per-Turn SRF-Filtered Model.

1. **input** frequency of operation f_0, safety margin Δf
2. $[x_v]$.: design space sampling with DOE
$[f]$, $[y_m]$, $[SRF]$.: DOE simulated in ADS Momentum (Quasi-Monte-Carlo)
//training phase
3. **for** each turn-related variable i of u **do**
4. **for** each discrete value j of $x_v\{i(ur)\}$ **do**
5. **for** each sample l with j variable, $[x_v\{i(j)\}]$, **do**
6. **if** $SRF\{x_v(l)\} > f_0 + \Delta f$ **then**
7. add sample/component l to $[x_v]^*$, $[f]^*$ and $[y_m]^*$
8. **train** a per-turn model $SRF_{<u=i, \; ur=j>}$ to predict SRF
using the features $[x_{v-u}\{i(j)\}]$ and labels $[SRF \{ i(j)\}]$
9. **for** each turn-related variable i of u **do**
10. **for** each discrete value j of $x_v^*\{u(ur)\}$ **do**
11. **for** each frequency sampled η of f^* **do**
12. **for** each S-parameter t of y_m^* **do**
13. **train** a FI per-turn model S-Param$_{\{u=i, \; ur=j, \; s\}}$ using
$[x_{v-u}\{i(j)\}]^{*T}$, $f^*\{i(j)\}(\eta)$ and $[y_m\{i(j)\}]^{*T}$
//evaluation phase
14. **for** each c device of set C to be evaluated **do**
15. **if** $SRF_{<u(c), \; ur(c)>}\{x_v(c)\} < f_0 + \Delta f$ **then**
16. discard passive component c
else
predict $y_m\{c\}$ using S-Param$_{\{u(c), \; ur(c), \; f0\}}$

(a)   (b)
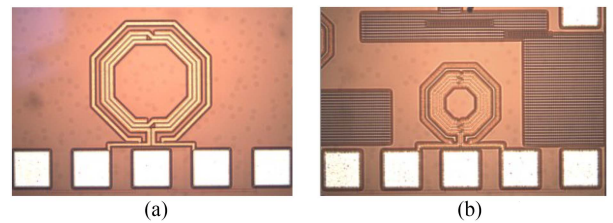
FIGURE 4. Two of the fabricated inductors used for experimental validation of the developed model. (a) Inductor 1 and (b) Inductor 2.

technique together with Strategy IV showed the best accuracy and complies with all bullet points described at the beginning of Section V. Therefore, this combination of technique and strategy is the one embedded in PACOSYT for the following experiments conducted on this paper.

F. VALIDATION OVER PHYSICAL PROTOTYPES
The ultimate validation of any modeling technique is the experimentation on physical prototypes. Previous sections have already shown the accuracy of the model vs. the reference EM simulation. In this section, further validation is pursued by using fabricated devices; in particular four different inductors (two of them shown in Fig. 4) have been fabricated in a 0.35μm CMOS technology. On-wafer characterization was performed using a Cascade Microtech M150 probe station and an Agilent N5230A network analyzer. Fig. 5(a)-(d) show the inductor performance parameters (inductance and quality

TABLE 6. Inductor Performances at 5 GHz. Experimental (E) Results Versus Full-Wave (EM) Simulations and Model (M) Estimation

Inductors	L_E (nH)	L_{EM} (nH)	EM-E (%)	L_M (nH)	M-E (%)	Q_E	Q_{EM}	EM-E (%)	Q_M	M-E (%)	SRF_E (GHz)	SRF_{EM} (GHz)	EM-E (%)	SRF_M (GHz)	M-E (%)
Inductor 1 (N=3 D_{IN}=187 μm w=8.8μm)	3.21	3.06	**4.65**	3.06	**4.63**	10.60	10.85	**2.35**	10.84	**2.25**	12.23	11.90	**2.70**	11.85	**3.11**
Inductor 2 (N=5 D_{IN}=84 μm w=5μm)	4.06	3.90	**3.99**	3.90	**3.98**	8.64	8.84	**2.24**	8.84	**2.30**	11.41	11.70	**2.54**	11.68	**2.37**
Inductor 3 (N=4 D_{IN}=119 μm w=6.95 μm)	3.61	3.45	**4.49**	3.45	**4.50**	9.70	10.09	**4.03**	10.09	**4.05**	11.56	11.50	**0.52**	11.53	**0.26**
Inductor 4 (N=5 D_{IN}=61 μm w=5.05 μm)	2.77	2.63	**5.03**	2.63	**5.05**	8.67	8.24	**4.99**	8.23	**5.11**	14.75	15.10	**2.38**	15.10	**2.37**
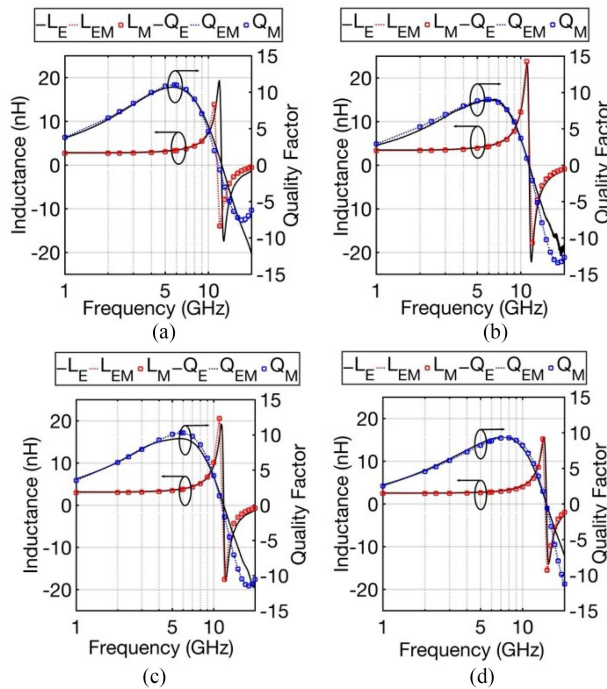
FIGURE 5. Performance comparison for the fabricated inductors. (a) Inductor 1, (b) Inductor 2, (c) Inductor 3, and (d) Inductor 4.

factor) comparison between the full- wave EM simulation (LEM and QEM), the experimental (LE and QE) and the model predictions (LM and QM), for the fabricated inductors. It is possible to observe that an exceptional matching between measurements and model predictions is achieved for the entire measured frequency range (up to 20 GHz).

Table 6 provides a more detailed analysis of the inductor performances at 5 GHz. In this Table, the fourth, ninth and fourteenth columns represent the error between the full-wave EM simulation and experimental measurements (EM-E (%)). The sixth, eleventh and sixteenth columns represent the error between the model and experimental measurements (M-E (%)) for L, Q and SRF, respectively. By observing such results, it is reasonable to conclude that the model provides an exceptionally reliable estimation of the inductor performance parameters: the model deviates less than 5% in L and Q (at 5 GHz) with respect to experimental measurements. The discrepancies attained are almost the same as the errors between full-wave EM simulations and measurements, suggesting that these small discrepancies are caused more by manufacturing variations than by significant errors in the model. Regarding

the SRF model prediction, it is, to the best of the authors' knowledge, the most accurate inductor SRF predictor available in the literature (with less than 3% error when compared to measurements).

G. STATE-OF-THE-ART COMPARISON

In Table 7 it is possible to observe a comparison against other inductor and transformer models available in the literature. Regarding the general applicability of the model, this work is the only one to successfully apply the same modeling technique and strategy to both inductors and transformers. Furthermore, regarding the design space modeled, it is the one that covers the wider design space for transformers (and the only one which covers 1:2 and 2:1 transformers) and a considerably wider design space than most approaches for inductors, while reaching higher frequencies than other works (200 GHz). This is a huge advantage of this model as it allows a wider design space search during component optimization and by being wideband and valid up to 200 GHz it allows accurate mm-Wave circuit simulations. Concerning model accuracy, this work provides the most accurate global model for both inductors and transformers. Also, this work is the only one to provide experimental data of physical prototypes. Apart from the other advantages mentioned in Table 7 (e.g., automated training data generation, having the layout readily available, not needing more EM data after model generation, etc.) two of the most important features are that the model developed in this work does not need any dedicated framework or closed-source licenses, and, therefore, it is possible to develop an open-source tool for the RF and mm-Wave design community to use.

V. PACOSYT: A PASSIVE COMPONENT SYNTHESIS TOOL

The architecture of the proposed tool, PACOSYT, is illustrated in Fig. 6. It comprises three main operation modes: model generation, passive component synthesis and passive component evaluation. The model generation mode allows the user to create models for different topologies or technologies beyond the ones already provided and shown in this work. For this, the user only has to provide a DOE for the new topology/ technology. The passive component synthesis mode is available because, typically, the design of such components can be seen as an optimization problem (e.g., the designer is looking for an inductor/transformer with a given L, with the maximum Q possible and the lowest area). PACOSYT uses an optimization algorithm to perform inductor/transformer automated design (i.e., synthesis), where the designer inputs the

TABLE 7. Inductor and Transformer Models State-of-the-Art Comparison

	This work	[9]	[13]	[11]	[16]	[17]	[18]	[20]	[24]
Maximum frequency[1]	200GHz	2.5GHz	35GHz	60GHz	10GHz	10GHz	10GHz	n/ment	150GHz
Inductor Geometry Covered (in μm except N)	$N=[1,5]$ $D_{IN}=[60,200]$ $w=[5,15]$	$N=2;4;6;8$ $D_{IN}=[100,340]$ $w=[4,32]$ $s=[1,5]$	$N=3$ $D_{IN}=$fixed $w=$fixed	$N=1;1.5$ $D_{IN}=[30,100]$ $w=[3,10]$ $s=[3,8]$	$N=3;4;5$ $D_{IN}=[40,160]$ $w=[2,20]$ $s=[1,10]$	$N=[1,8]$ $D_{IN}=[20,200]$ $w=[5,15]$	$D_{IN}=[60,180]$ $w=[2.5,25]$	n/mod	n/mod
Maximum MAPE - Model vs. EM (Inductor)	0.15%	5%	<-60dB (for Spar.)[3]	n/avail[4]	4.6%	0.88%	17%		
Maximum MAPE - Model vs. Measures (Inductor)	4.65%	n/avail	n/avail	n/avail	n/avail	n/avail	n/avail	n/avail	n/avail
Transformer Geometry Covered (in μm except N)	$N=1:1;2:1;1:2$ $D_{IN}=[30,200]$ $w=[5,15]$	n/avail	n/avail	$N=1:1$ $D_{IN}=[20,150]$ $w=[5,10]$	n/avail	n/avail	n/mod	$N=1:1$ D_{IN} and w n/ment	$N=1:1$ $D_{IN}=[20,100]$ $w=[5,10]$
Maximum MAPE - Model vs. EM (Transformer)	1.94%			n/avail[4]				15%	5.7%
Experimental results	yes	no	no	no	no	no	no	no	no
Model inputs	N, D_{IN}, w	N, D_{IN}, w, s	Area[2]	N, D_{IN}, w	N, D_{IN}, w, s	N, D_{IN}, w	L and Q	L and Q	D_{IN}, w
Models SRF directly	yes	yes	no	no	no	yes	no	yes	yes
Technique	RBF	ANN	PM	GP	GP	GP	ANN	ANN	GP
Tailored strategy	yes	no	yes	yes	yes	yes	no	no	Yes
Automated training data generation	yes	n/ment	yes	yes	n/ment	no	n/ment	n/ment	No
Needs EM simulation after initial model	no	no	yes[3]	yes[5]	yes[6]	no	yes[6]	no	No
Scalable to different structures	yes	n/shown	yes	yes	n/shown	n/shown	n/shown	n/shown	n/shown
Scalable to different technologies	yes	n/shown	n/shown	n/shown	n/shown	n/shown	n/shown	n/shown	n/shown
Component optimization	yes	yes	no	yes	yes	yes	no	no	yes
Layout readily available	yes	yes	yes	yes	yes	yes	yes	yes	yes
Integrated in tool for design	yes	no	no	no	no	no	no	no	no
Integrated in tool for optimization	yes	no	no	no	no	no	no	no	no
Usage of dedicated framework	no	no	yes	yes	yes	yes	no	yes	yes
Using only open-source software[7]	yes	no	no	no	no	no	yes	yes	no

[1]At which the model error is evaluated (at least graphically); [2]N and w are fixed (D_{IN} varies accordingly to the area);
[3]It is an adaptative model, and therefore new samples are iteratively added until the error constraint is met;
[4]In Surrogate assisted method, the component used is always electromagnetically simulated, therefore the error is 0%;
[5]Surrogate assisted method; [6]Design refinements are performed by adding more EM samples after the multi-objective optimization is done
[7]For model creation/usage. Except for evaluating the performances of the training samples (all works in the Table use an EM simulator)
n/avail not available; **n/shown** not shown; **n/ment** not mentioned; **n/mod** not modeled
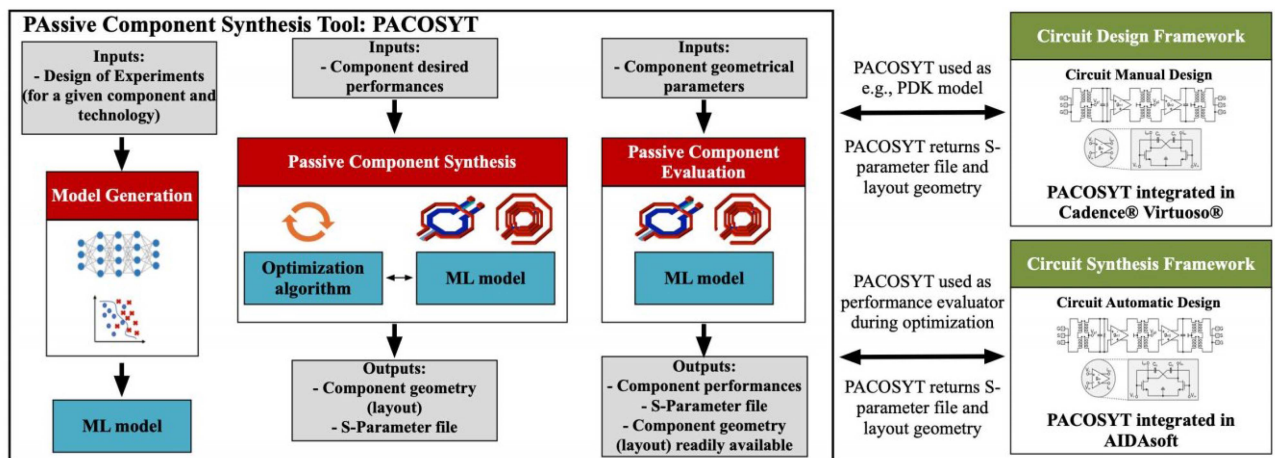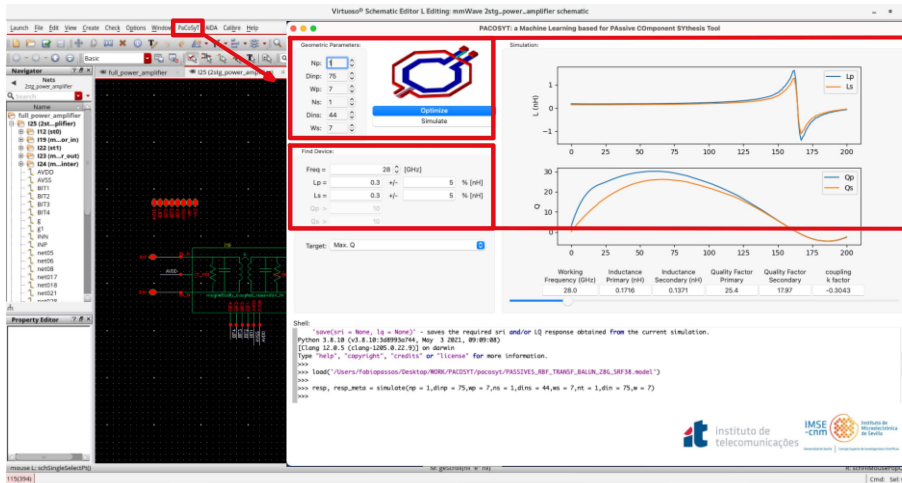

FIGURE 6. PACOSYT's architecture with its two operation modes (component synthesis and component evaluation) and also its integrability in frameworks for circuit manual design and circuit automatic design.

FIGURE 7. PACOSYT GUI integrated in Cadence Virtuoso with its dedicated menu inside Cadence framework.

desired inductance, and the component with the highest quality factor and lowest area is outputted by PACOSYT. Also, the component geometry (i.e., layout) is readily available. On the other operation mode (passive component evaluation), PACOSYT allows the user to input the component geometrical parameters (e.g., N, DIN, w for inductors), and the tool outputs the performances (L, Q, etc.) and the S-parameter file for circuit simulation. This mode is similar to how a designer would use a foundry PDK model. However, PACOSYT has the advantage of being useful up to higher frequencies (i.e., 200 GHz) than typical PDK models (e.g., 20/30 GHz), has EM accuracy (less than 2% error when compared to full-wave EM simulations), and is faster to evaluate components than an EM simulation (in milliseconds rather than minutes), as will be shown in this section.

The developed tool, PACOSYT has its GUI shown in Fig. 7. Moreover, Fig. 7 also shows how the tool is integrated into Cadence Virtuoso for seamlessly use by circuit designers. However, the tool itself runs standalone and does not require any closed-source license to operate. In the next two subSections, both modes used to synthesize/design components are illustrated.

A. PASSIVE COMPONENT EVALUATION

By integrating PACOSYT into a design framework, it can be used as any PDK model, and since the tool provides the S-parameter file immediately, it can be directly used in circuit simulations. In this example, the inductor with the following geometry was simulated in the tool: N=2, Din=110μm, w=7μm. The simulation of the inductor took approximately 0.2 seconds and its performances can be seen directly in the tool (as shown in Fig. 7). As a model validation process, the inductor was simulated electromagnetically to evaluate the error between the model and the EM simulation. The comparison is shown in Fig. 8(the inductor layout can also be seen) where it is possible to observe an excellent accuracy up to 200GHz, even achieving a perfect matching after the second
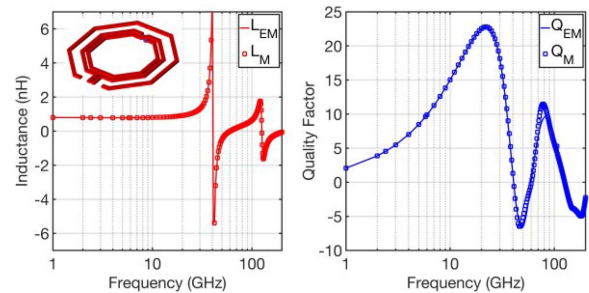

FIGURE 8. Performance comparison between the model and EM simulation for the inductor with N=2, Din=110μm, w=7μm. The layout of the simulated inductor can also be seen.

SRF frequency (at 5GHz the relative error is 0.38% in L and 0.31% in Q). The EM simulation of this inductor took approximately 24 minutes to run. Since the model took 0.2 seconds to evaluate the same inductor in the same frequency points, it is an efficiency improvement of 12000%. This efficiency improvement can be even superior if the inductor has a higher number of turns, as the EM simulation time exponentially increases with the complexity of the component and the model evaluation time is the same for every structure.

B. PASSIVE COMPONENT OPTIMIZATION

Another advantage of the tool is that it provides the possibility to perform inductor/transformer synthesis using an optimization algorithm. Hence, the designer can just define the desired inductance and the tool finds the passive component with the highest quality factor or smallest area.

As an example, a transformer optimization is formulated as:

$$Maximize\ Q_P\ and\ Q_S\ @28GHz$$

$$Such\ that \begin{cases} L_P = 370pH \pm 10pH\ @\ 28GHz \\ L_S = 220pH \pm 10pH\ @\ 28GHz \\ k = -0.3 \pm 0.1\ @\ 28GHz \\ SRF_P\ and\ SRF_S > 38GHz \end{cases} \quad (7)$$
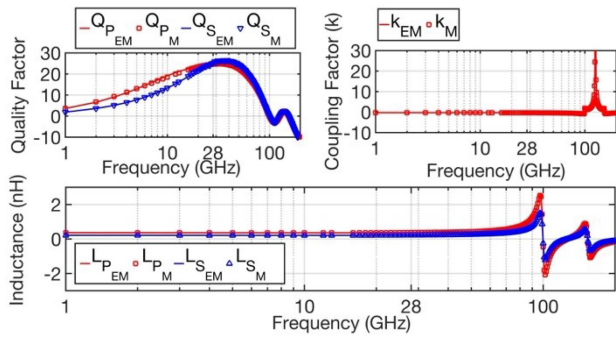
FIGURE 9. Performance comparison between the model and EM simulation of the transformer with NP=NS=1, DinP=140μm, DinP=82μm, wS=5μm and wS=13.5μm. The layout of the transformer can also be seen.

In PACOSYT, the optimization algorithm implemented is a version of the selection-based differential evolution [38] in Python. The optimization was executed with 50 individuals and 200 generations, and the obtained transformer had the following parameters: NP=NS=1, DinP=140μm, DinP=82μm, wS=5μm and wS=13.5μm. The comparison between the model and the EM simulation of the same transformer is shown in Fig. 9 for all the performances of interest (the transformer layout can also be seen). It can be observed that a perfect matching is achieved for all performances from low frequencies up to 200GHz, with an exceptional accuracy across the entire frequency range and even managing to accurately model the second SRF point for both the primary and secondary. Moreover, the relative error at 28 GHz is 0.21% in LP, 0.15% in QP, 0.14% in LS, 0.26% in QS and 0.19% in k. It can be concluded that this is a suitable model for circuit simulations, due to its wideband capacity. Even if the designer is working with an operating frequency of 28 GHz, it is crucial to have models valid up to two or three times the operating frequency for circuits where the second and third harmonics are important.

The entire optimization took around 4 minutes to evaluate 10000 transformers and reach an optimal one. The time needed to simulate electromagnetically only one transformer (the one obtained in the optimization) was 16 minutes. Therefore, if the EM simulator was used as a performance evaluator in the optimization instead of the model, the time needed to perform the optimization (simulating 10000 transformers) would be around 160000 minutes, approximately 111 days. Therefore, it is clear the advantage of using the model during the design stage, as the accuracy is maintained but allied with efficiency.

From the experiments in this section, it can be concluded that when designing optimal passives in an automated synthesis process using optimization algorithms (where thousands of transformers are evaluated), using an EM simulator is simply unbearable. Hence, the surrogate model becomes the only solution.

VI. POWER AMPLIFIER AUTOMATED SYNTHESIS

In this Section, PACOSYT was integrated with AIDAsoft, an optimization tool capable of automatically tackling circuit
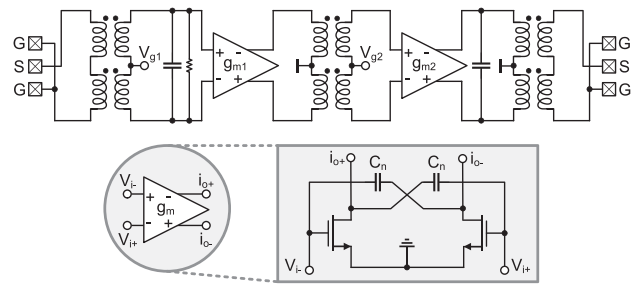

FIGURE 10. Power amplifier topology used for illustrating the usage of PACOSYT together with AIDASoft for circuit optimization.
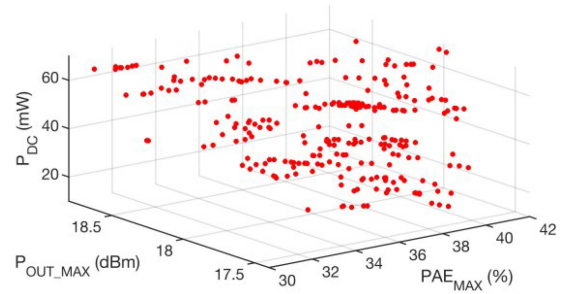

FIGURE 11. POF of the PA achieved using AIDASoft for circuit optimization and PACOSYT for the transformer evaluation.

sizing and layout, including process variability [39], [40]. In this tool, the user selects the desired circuit objectives and constraints, and using a multi-objective optimization algorithm, the tool searches for the best circuit sizing solutions that comply with selected specifications. Multi-objective optimization algorithms allow to simultaneously consider several design objectives during the optimization, and the result of the optimization is a set of solutions, the Pareto optimal front (POF), exhibiting the best trade-offs between these objectives. In this example, the objective was to optimize the PA of Fig. 10, operating in the band of 26.5∼30 GHz in a 65 nm CMOS technology and using a supply voltage VDD=1.2V.

The PA uses 3 transformers evaluated during the circuit optimization using the models in PACOSYT. The optimization was performed with 300 individuals and 150 generations with the specifications shown in the first two columns of Table 8. The design objectives of the optimization were: maximization of the maximum power-added efficiency (PAEMAX) and maximum output power (POUT_MAX) and minimization of the power consumption at DC (PDC). The circuit optimization took 56 hours to complete. Its output, i.e., the POF, comprises 300 different PAs, and is shown in Fig. 11. Each dot of this figure represents the performances of a different PA with its sizing fully defined and the transformers evaluated with PACOSYT.

From the 300 achieved designs, one was selected for simulation in Cadence Virtuoso. The selected PA has a saturated output power of 18.11dBm, a peak PAE of 38% and 18.8dB small-signal gain, which are very good performances when compared to the state-of-the-art for the single path power PA topologies in similar technology nodes [41].

TABLE 8. Specifications for the PA optimization. Comparison Between PA Performances Using PACOSYT and EM Simulator for a Given PA Design

PA Performance	PA Specifications	Performances of Selected PA @ 28 GHz (PACOSYT)	Performances of Selected PA @ 28 GHz (Transf. EM simulated)	Error (%)
S_{11} @ 26.5-30 GHz	< -12 dB	-20.102 dB	-20.056 dB	0.087
S_{22} @ 26.5-30 GHz	< -5 dB	-5.850 dB	-5.856 dB	0.230
S_{21} @ 26.5-30 GHz	> 12 dB	18.885 dB	18.881 dB	0.020
S_{21} Variation (@ 26.5-30 GHz)	< 1.7dB	Complies with spec.	Complies with spec.	-
Rollet Stb Factor @ 1Hz-120GHz	> 1	Complies with spec.	Complies with spec.	-
P_{DC}	Minimize (< 70 mW)	33.9874 mW	33.9877 mW	0.001
P_{OUT_MAX}	Maximize (> 8 dBm)	18.11 dBm	18.12 dBm	0.055
PAE_{MAX}	Maximize (> 20%)	38.08 %	38.04%	0.105
Power Gain$_{MAX}$	> 12 dB	18.88 dB	18.89 dB	0.052
P_{1dB}	> 10 dBm	14.128 dBm	14.125 dBm	0.021

(a)

(b)

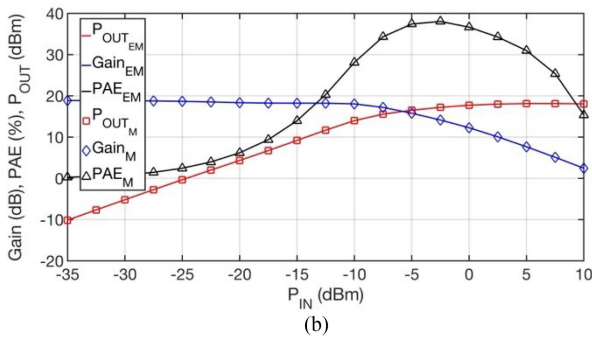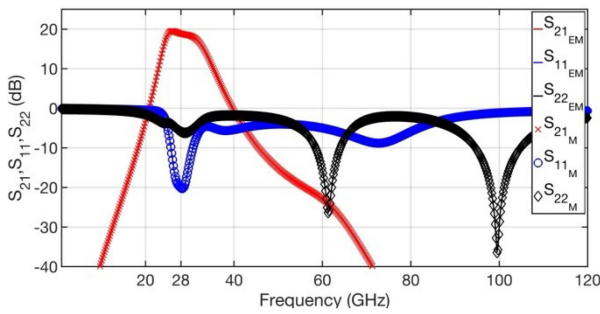**FIGURE 12.** Performance comparison of the synthesized PA: (a) Gain and input matching. S11M, S21M and S22M represent the performances of the PA with the transformers simulated with PACOSYT and S11EM, S21EM and S22EM represent the performances of the PA with the transformers electromagnetically simulated. (b) Output power (POUT), Gain and PAE as a function of the input power (PIN), with the same notation as in a).

FIGURE 13. Passive component floorplan of the selected PA with the PADs and bias lines already set (missing the active stages and two capacitances in the input and output stage).

optimization. Hence, it is possible to remove the EM simulator for the design of passive components, making the design stage much more efficient. Furthermore, in this optimization 135000 transformers were simulated (i.e., 300 individuals × 150 generations × 3 transformers per circuit), something that is completely impossible to perform with an EM simulator, as it would amount to approximately 467 days of optimization time (assuming that each transformer takes around 15 minutes to simulate electromagnetically). Therefore, in this section, the value of the developed model and tool is proven once again both for efficiency and accuracy.

Moreover, in mm-Wave circuits, the layout highly depends on the passive components. Since, with PACOSYT, the geometry of the passives is readily available, having a floorplan for the desired circuit is immediate. Fig. 13 shows the floorplan of the circuit with the performances shown in Fig. 12 (without the active stages).

All tools (AIDAsoft, PACOSYT, and Cadence Virtuoso) are completely integrated, so transferring a design between AIDAsoft and Virtuoso is immediate. To inspect the PA performance deviations due to the PACOSYT model errors, all the transformers in the chosen PA design were EM simulated, and the PA was re-simulated. The performance deviations between using PACOSYT or using a full-wave EM simulator are depicted in Fig. 12 and detailed in columns three to five of Table 8 for the frequency of 28 GHz. It is possible to conclude that these deviations are negligible (below 0.23%), demonstrating that PACOSYT provides an extremely fast and accurate simulation model for circuit design and
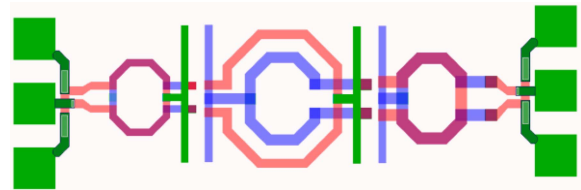
VII. CONCLUSION

In this work, the application of different supervised ML techniques and modeling strategies for integrated inductors and transformers was examined. It was possible to develop an extremely accurate model using the RBF technique together with smart modeling strategies, resulting in performance values with less than 2% error when compared to full-wave electromagnetic simulations and also less than 5% when compared to experimental measurements. A tool, named PACOSYT, was developed enabling user-friendly model creation and evaluation. It also integrates the model and an optimization algorithm which allows synthesizing passive

components in minutes with electromagnetic accuracy and optimal performances. The tool was also integrated into Cadence Virtuoso and AIDASoft for circuit design and optimization. With such a range of tools, it is possible to design hundreds of circuits in a couple of days with optimal performances and excellent accuracy in the passive design from an initial design stage. This fact highly helps to reduce the design iterations and aims at a first-pass fabrication success. All the data presented in this work, as well as the PACOSYT tool, is available online in a public repository.

REFERENCES

[1] C. Doan, S. Emami, A. Niknejad, and R. Brodersen, "Millimeter-wave CMOS design," *IEEE J. Solid-State Circuits*, vol. 40, no. 1, pp. 144–155, Jan. 2005.

[2] F. Passos, M. H. Fino, E. Roca, R. González-Echevarría, and F. V. Fernández, "Lumped element model for arbitrarily shaped integrated inductors: A statistical analysis," in *Proc. IEEE Int. Conf. Microw., Commun., Antennas Electron. Syst.*, 2013, pp. 1–5.

[3] Y. Tsai and T. Horng, "Wideband compact PI equivalent circuit for modeling on-chip spiral inductors," *IEEE Microw. Wireless Compon. Lett.*, vol. 22, no. 1, pp. 26–28, Jan. 2012.

[4] C. Wang et al., "A wideband predictive double-pi equivalent-circuit model for on-chip spiral inductors," *IEEE Trans. Electron Devices*, vol. 56, no. 4, pp. 609–619, Apr. 2009.

[5] J. Brinkhoff, D. Pham, K. Kang, and F. Lin, "A new six-port transformer modeling methodology applied to 10-dBm 60-GHz CMOS ASK modulator designs," *IEEE Trans. Microw. Theory Techn.*, vol. 58, no. 2, pp. 297–309, Feb. 2010.

[6] D. Hou et al., "Distributed modeling of six-port transformer for millimeter-wave SIGE BiCMOS circuits design," *IEEE Trans. Microw. Theory Techn.*, vol. 60, no. 12, pp. 3728–3738, Dec. 2012.

[7] Z. Gao et al., "A broadband and equivalent-circuit model for millimeter-wave on-chip M:N six-port transformers and baluns," *IEEE Trans. Microw. Theory Techn.*, vol. 63, no. 10, pp. 3109–3121, Oct. 2015.

[8] S. Koziel and J. W. Bandler, "Space-mapping optimization with adaptive surrogate model," *IEEE Trans. Microw. Theory Techn.*, vol. 55, no. 3, pp. 541–547, Mar. 2007.

[9] S. K. Mandal, S. Sural, and A. Patra, "ANN- and PSO-based synthesis of on-chip spiral inductors for RF ICs," *IEEE Trans. Comput.-Aided Des. Integr. Circuits Syst.*, vol. 27, no. 1, pp. 188–192, Jan. 2008.

[10] D. Gorissen, I. Couckuyt, P. Demeester, T. Dhaene, and K. Crombecq, "A surrogate modeling and adaptive sampling toolbox for computer based design," *J. Mach. Learn. Res.*, vol. 11, pp. 2051–2055, 2010.

[11] B. Liu, D. Zhao, P. Reynaert, and G. Gielen, "Synthesis of integrated passive components for high-frequency RF ICs based on evolutionary computation and machine learning techniques," *IEEE Trans. Comput.-Aided Des. Integr. Circuits Syst.*, vol. 30, no. 10, pp. 1458–1468, Oct. 2011.

[12] M. B. Yelten, T. Zhu, S. Koziel, P. D. Franzon, and M. B. Steer, "Demystifying surrogate modeling for circuits and systems," *IEEE Circuits Syst. Mag.*, vol. 12, no. 1, pp. 45–63, Firstquarter 2012.

[13] F. Ferranti, L. Knockaert, T. Dhaene, and G. Antonini, "Parametric macromodeling based on amplitude and frequency scaled systems with guaranteed passivity," *Int. J. Numer. Modelling*, vol. 25, pp. 139–151, 2012.

[14] N. Leszczynska, I. Couckuyt, T. Dhaene, and M. Mrozowski, "Low-cost surrogate models for microwave filters," *IEEE Microw. Wireless Compon. Lett.*, vol. 26, no. 12, pp. 969–971, Dec. 2016.

[15] J. Xu and D. E. Root, "Artificial neural networks for compound semiconductor device modeling and characterization," in *Proc. IEEE Compound Semicond. Integr. Circuit Symp.*, 2017, pp. 1–4.

[16] S. Koziel, P. Kurgan, and J. W. Bandler, "Multi-objective mixed-integer design optimization of planar inductors using surrogate modeling techniques," in *Proc. IEEE MTT-S Int. Microw. Symp.*, 2017, pp. 1632–1634.

[17] F. Passos, E. Roca, R. Castro-Lopez, and F. V. Fernandez, "Radio-frequency inductor synthesis using evolutionary computation and Gaussian-process surrogate modeling," *Appl. Soft Comp.*, vol. 60, pp. 495–507, 2017.

[18] N. Dervenis, G. Alexandridis, and A. Stafylopatis, "Neural network specialists for inverse spiral inductor design," in *Proc. IEEE Int. Conf. Tools Artif. Intell.*, 2018, pp. 60–64.

[19] W. Na, W. Zhang, S. Yan, and G. Liu, "Automated neural-based modeling of microwave devices using parallel computation and interpolation approaches," *IEEE Access*, vol. 7, pp. 73929–73937, 2019.

[20] D. Munzer et al., "Residual network based direct synthesis of EM structures: A study on one-to-one transformers," in *Proc. IEEE Radio Freq. Integr. Circuits Symp.*, 2020, pp. 143–146.

[21] J. Zhang, J. Chen, Q. Guo, W. Liu, F. Feng, and Q.-J. Zhang, "Parameterized modeling incorporating MOR-based rational transfer functions with neural networks for microwave components," *IEEE Microw. Wireless Compon. Lett.*, vol. 32, no. 5, pp. 379–382, May 2022.

[22] S. Koziel and M. Abdullah, "Machine-learning-powered EM-based framework for efficient and reliable design of low scattering meta-surfaces," *IEEE Trans. Microw. Theory Techn.*, vol. 69, no. 4, pp. 2028–2041, Apr. 2021.

[23] W. Zhang et al., "Surrogate-assisted multistate tuning-driven EM optimization for microwave tunable filter," *IEEE Trans. Microw. Theory Techn.*, vol. 70, no. 4, pp. 2015–2030, Apr. 2022.

[24] F. Passos, E. Roca, J. Sieiro, R. Castro-Lopez, and F. V. Fernandez, "An efficient transformer modeling approach for mm-wave circuit design," *AEU - Int. J. Electron. Commun.*, vol. 128, 2021, Art. no. 153496.

[25] J. Jin, F. Feng, J. Zhang, J. Ma, and Q.-J. Zhang, "Efficient EM topology optimization incorporating advanced matrix Padé via Lanczos and genetic algorithm for microwave design," *IEEE Trans. Microw. Theory Techn.*, vol. 69, no. 8, pp. 3645–3666, Aug. 2021.

[26] A. Pietrenko-Dabrowska and S. Koziel, "Surrogate modeling of impedance matching transformers by means of variable-fidelity electromagnetic simulations and nested cokriging," *Int. J. RF Microw. Comput.-Aided Eng.*, vol. 30, 2020, Art. no. e22268.

[27] S. Koziel and A. Pietrenko-Dabrowska, "Efficient gradient-based algorithm with numerical derivatives for expedited optimization of multi-parameter miniaturized impedance matching transformers," *Radioengineering*, vol. 27, pp. 572–578, 2019.

[28] J. E. Rayas-Sánchez, S. Koziel, and J. W. Bandler, "Advanced RF and microwave design optimization: A journey and a vision of future trends," *IEEE J. Microwaves*, vol. 1, no. 1, pp. 481–493, Jan. 2021.

[29] Accessed: Jul. 27, 2022. [Online]. Available: https://www.cadence.com/ko_KR/home/tools/custom-ic-analog-rf-design/circuit-design/virtuoso-analog-design-environment.html

[30] N. Lourenço, R. Martins, and N. Horta, *Automatic Analog IC Sizing and Optimization Constrained With PVT Corners and Layout Effects*. Berlin, Germany: Springer, 2017.

[31] Accessed: Jul. 27, 2022. [Online]. Available: http://aidasoft.com/Home

[32] Accessed: Jul. 27, 2022. [Online]. Available: https://github.com/nunocclourenco/pacosyt

[33] K. Okada and K. Masu, "Modeling of spiral inductors," in *Advanced Microwave Circuits and Systems*. Berlin, Germany: Springer, 2010, pp. 291–312.

[34] D. A. Frickey, "Conversions between S, Z, Y, H, ABCD, and T parameters which are valid for complex source and load impedances," *IEEE Trans. Microw. Theory Techn.*, vol. 42, no. 2, pp. 205–211, Feb. 1994.

[35] Accessed: Jul. 27, 2022. [Online]. Available: https://www.keysight.com/zz/en/products/software/pathwave-design-software/pathwave-advanced-design-system.html

[36] K. P. Murphy, *Probabilistic Machine Learning: An Introduction*. Cambridge, MA, USA: MIT Press, 2022.

[37] M. Bauer, M. Wilk, and C. Rasmussen, "Understanding probabilistic sparse Gaussian process approximations," in *Proc. Int. Conf. Neural Inf. Process. Syst.*, 2016, Art. no. 29.

[38] K. Zielinski and R. Laur, "Constrained single-objective optimization using differential evolution," in *Proc. IEEE Int. Conf. Evol. Comput.*, 2006, pp. 223–230.

[39] L. Mendes, J. Vaz, F. Passos, N. Lourenço, and R. Martins, "In-depth design space exploration of 26.5-to-29.5-GHz 65-nm CMOS low-noise amplifiers for low-footprint-and-power 5G communications using One-and- Two -step design optimization," *IEEE Access*, vol. 9, 9, pp. 70353–70368, 2021.

[40] R. Martins et al., "Design of a 4.2-to-5.1 GHz ultralow-power complementary class-B/C hybrid-mode VCO in 65-nm CMOS fully supported by EDA tools," *IEEE Trans. Circuits Syst. I, Reg. Papers*, vol. 67, no. 11, pp. 3965–3977, Nov. 2020.

[41] C. Yu, J. Feng, and D. Zhao, "A 28-GHz CMOS broadband single-path power amplifier with 17.4-dBm P1dB for 5G phased-array," in *Proc. IEEE 44th Eur. Solid State Circuits Conf.*, 2018, pp. 38–41.

RICARDO MARTINS (Member, IEEE) received the Ph.D. degree in electrical and computer engineering from the Instituto Superior Técnico – University of Lisbon, Lisbon, Portugal, in 2015. Since 2011, he has been with the Instituto de Telecomunicações, developing electronic design automation tools, where he holds a Postdoctoral Research position. He has authored or coauthored more than 80 publications, including books, international journals, and conferences papers. His research interests include electronic design automation tools for analog, mixed-signal, radio-frequency and millimeter wave integrated circuits, deep nanometer integration technologies, and applied soft computing, machine and deep learning. He was the General Chair of the International Conference on SMACD 2019 and a member of the organizing committee of several other conferences, such as IEEE ICECS, PRIME, and NGCAS.

FÁBIO PASSOS (Senior Member, IEEE) received the Ph.D. degree from the Universidad de Sevilla, Seville, Spain, in 2018. In 2018, he was conducting his work with the Instituto de Microelectrónica de Sevilla (IMSE-CNM), Seville. He was with several Academic and industrial institutions, such as Analog Devices, Dialog Semiconductors, IMEC, Instituto de Telecomunicações, and University of Barcelona, Barcelona, Spain. He has collaborated in several international research projects as part of the research team or as PI. His research interests include the development of automated design methodologies for RF and mm-Wave circuits. He is currently a Research Fellow with Instituto de Telecomunicações having received a Postdoctoral Marie Skłodowska-Curie Individual Fellowship. He was the recipient of several best paper awards, EDA Competition Award in SMACD 2016, and Prestigious Outstanding Dissertation Award from the European Design and Automation Association, in 2019.

RAFAEL CASTRO-LÓPEZ received the M.S. degree in electronic physics (Licenciado en Física Electrónica degree) and the Ph.D. degree (Doctor en Ciencias Físicas) from the University of Seville, Seville, Spain, in 1998 and 2005, respectively. Since 1998, he has been with the Institute of Microelectronics of Seville (CSIC-IMSE-CNM), where he currently holds the position of Tenured Scientist. He has participated in several national and international R&D projects and co-authored more than 100 international scientific publications, including journals, conference papers, and book chapters. His research interests include integrated circuits, especially design and computer-aided design for analog, and mixed-signal circuits.

NUNO LOURENÇO (Member IEEE) received the Licenciado, M.Sc., and Ph.D. degrees in electrical and computer engineering from the Instituto Superior Técnico, University of Lisbon, Lisbon, Portugal, in 2005, 2007, and 2014, respectively. Since 2005, he has been with the Instituto de Telecomunicaçes, Lisbon, where he currently holds a research position. He has coauthored more than 90 international scientific publications, including patents, books, journals, and conference papers. His research interests include AMS/RF IC design and artificial intelligence (Evolutionary computation and machine learning) applied to electronic design automation. Dr. Lourenço was the General Chair of SMACD 2022 and was involved in the Organizing committee of other international conferences, such as IEEE ISCAS or PRIME.

NUNO HORTA (Senior Member, IEEE) received the Licenciado, M.Sc., Ph.D., and Habilitation degrees in electrical engineering from Instituto Superior Técnico (IST), University of Lisbon, Lisbon, Portugal, in 1989, 1992, 1997, and 2014, respectively. In March 1998, he joined the IST Electrical and Computer Engineering Department. Since 1998, he has also been with the Instituto de Telecomunicações, where he is the Head of the Integrated Circuits Group. He has supervised more than 90 post-graduation works between M.Sc. and Ph.D. theses. He has authored or coauthored more than 150 publications as books, book chapters, international journals papers, and conferences papers. His research interests include analog and mixed-signal IC design, analog IC design automation, soft computing, and data science.

ELISENDA ROCA received the Ph.D. degree in physics from the Universidad de Barcelona, Barcelona, Spain, in 1995. Since 1995, she has been with the Instituto de Microelectrónica de Sevilla (IMSE, CSIC - Universidad de Sevilla), Seville, Spain, where she is currently a Tenured Scientist. She has been involved in different national and international research projects, and coauthored more than 250 papers in international journals, books, and conference proceedings. Her research interests include advance design methodologies for analog, mixed-signal, and RF integrated circuits, and characterization, mitigation and exploitation of variability of integrated devices and circuits.

FRANCISCO V. FERNÁNDEZ received the Ph.D. degree in microelectronics from the Universidad de Sevilla, Sevilla, Spain, in 1992. In 1993, he was a Postdoctoral Research Fellow with Katholieke Universiteit Leuven, Leuven, Belgium. From 1995 to 2009, he was an Associate Professor with the Department of Electronics and Electromagnetism, Universidad de Sevilla, where he was promoted to a Full Professor in 2009. He has authored or edited five books and has coauthored more than 250 papers in international journals and conferences. His research interests include microelectronic device and circuit reliability, and design and design methodologies of analog, mixed-signal, and RF circuits. He was the General Chair of three international conferences and regularly serves at the Program Committee of several international conferences. He has also participated as researcher or main researcher in numerous national and international R&D projects. He was the Editor-in-Chief of *Integration* and *VLSI Journal* (Elsevier) from 2005 to 2015.